ORIGINAL RESEARCH

Quantification of Myocardial Blood Flow Using Low-Dose Dynamic 320-row Multi-detector CT as Compared With ^{15}O-H_2O PET

Yasuka Kikuchi, M.D.[1]; Noriko Oyama-Manabe, M.D., Ph.D.[1]; Masanao Naya, M.D., Ph.D.[2]; Osamu Manabe, M.D., Ph.D.[3]; Yuuki Tomiyama, MS[3]; Tsukasa Sasaki, RT[4]; Chietsugu Katoh, M.D., Ph.D.[5]; Kohsuke Kudo, M.D., Ph.D.[1]; Nagara Tamaki, M.D., Ph.D.[3]; Hiroki Shirato, M.D., Ph.D.[6]

[1] Department of Diagnostic and Interventional Radiology, Hokkaido University Hospital, Sapporo, Japan

[2] Department of Cardiovascular Medicine, Hokkaido University Graduate School of Medicine, Sapporo, Japan

[3] Department of Nuclear Medicine, Hokkaido University Graduate School of Medicine, Sapporo, Japan

[4] Department of Radiology, Hokkaido University Hospital, Sapporo, Japan

[5] Hokkaido University Faculty of Health Sciences, Sapporo, Japan

[6]Department of Radiation Medicine, Hokkaido University Graduate School of Medicine, Sapporo, Japan

Corresponding Author

Noriko Oyama-Manabe

Department of Diagnostic and Interventional Radiology, Hokkaido University Hospital, Sapporo, Japan

Kita15, Nishi 7, kita-ku, Sapporo 060–8638, Japan

Phone: +81-11-706-5977, Fax: +81-11-706-7876

e-mail: norikooyama@med.hokudai.ac.jp

Abstract

Objectives: This study introduces a method to calculate myocardium blood flow (MBF) and coronary flow reserve (CFR) using the relatively low-dose dynamic 320-row multi-detector computed tomography (MDCT), validates the method against ^{15}O-H_2O positron-emission tomography (PET) and assesses the CFRs of coronary artery disease (CAD) patients.

Methods: Thirty-two subjects underwent both dynamic CT perfusion (CTP) and PET perfusion imaging at rest and during pharmacological stress. In 12 normal subjects (pilot group), the calculation method for MBF and CFR was established. In the other 13 normal subjects (validation group), MBF and CFR obtained by dynamic CTP and PET were compared. Finally, the CFRs of CTP and PET obtained by dynamic CTP and PET were compared between the validation group and CAD patients (n = 7).

Results: Correlation between MBF of MDCT and PET was strong ($r = 0.95$, $p<0.0001$). CFR showed good correlation between dynamic CTP and PET ($r = 0.67$, $p = 0.0126$). CFR_{CT} in the CAD group (2.3 ± 0.8) was significantly lower than that of in the validation group (5.2 ± 1.8) ($p = 0.0011$).

Conclusion: We established a method for measuring MBF and CFR with the relatively low-dose dynamic MDCT. Lower CFR was well demonstrated in CAD patients by

dynamic CTP.

Key Points

- MBF and CFR can be calculated using dynamic CTP with 320-row MDCT.
- MBF and CFR showed good correlation between dynamic CTP and PET.
- Lower CFR was well demonstrated in CAD patients by dynamic CTP.

Keywords MDCT・Cardiac・Perfusion・Myocardium blood flow・Coronary flow reserve

Introduction

Cardiac computed tomography angiography (CCTA) provides morphological information concerning coronary artery stenosis with high sensitivity and negative predictive value [1], but the degree of coronary obstruction assessed by CCTA remains a modest predictor of functional myocardial ischemia [2].

Measurements of myocardial blood flow (MBF) and coronary flow reserve (CFR) have been reported to be superior for evaluating the physiological significance of coronary lesion [3]. In patients with coronary artery disease (CAD), the reduction in CFR is proportional to the severity of myocardial ischemia [3]. Camici et al. reported that CFR reflects the ability of microvasculature to respond to stimuli and presumably small vessel function [3]. Even patients with angiographically normal arteries sometimes exhibit microvascular dysfunction and low CFR. CFR may therefore be useful for predicting flow-limiting disease [4]. Previous studies have reported a CFR < 2.0 reflects severe coronary artery stenosis, physiological myocardial ischemia, and microcirculatory dysfunction [5-8]. On the other hand, Kawata et al. has reported a CFR < 2.5 is useful for predicting outcome or microcirculatory dysfunction [9].

The extraction fraction of major tracers such as ammonia and rubidium for quantitative MBF and CFR assessment are lower than that of ^{15}O-H_2O PET [10]. ^{15}O-H_2O positron-emission tomography (PET) is the gold standard tracer because it

employs a freely diffusible tracer with 100 % extraction fraction even at high blood flow [10]. However, its clinical use is limited because a cyclotron is required and morphological coronary artery imaging is impossible.

CT perfusion (CTP) combined with coronary CCTA (CTP/CCTA) shows promise for the accurate detection of obstructive atherosclerosis causing myocardial ischemia [11,12]. CTP/CCTA provides self-registered datasets permitting direct correlation of stenosis with downstream perfusion deficits [13-15]. Quantitative dynamic CTP requires data for several cardiac cycles, resulting in a high radiation dose. Given recent advances in multi-detector computed tomography (MDCT) technology [16], we considered that a novel 320-row MDCT scanner might permit quantitative, low-dose, whole MBF measurement in a single heartbeat without significant artifacts.

The present study was conducted to establish a method for calculating whole MBF and CFR using low-dose dynamic 320-row MDCT (MBF_{CT}, CFR_{CT}), with validation against ^{15}O-H_2O PET (MBF_{PET}, CFR_{PET}) as the gold standard, and to compare CFRs in normal subjects and patients with CAD.

Materials and Methods

Subjects

This study was prospective. Our institutional review board approved this study from August to December, 2012. Written informed consent was obtained from all subjects.

Thirty volunteers (30-55 years old), with no history, family history, symptoms, or clinical evidence of CAD (2 eventually excluded because the MDCT protocol was not completed) and 4 patients with symptoms or risk factors of CAD were recruited. A normal group without significant coronary stenosis (< 50 %) and a CAD group with significant coronary stenosis (≥ 50 %) were identified based on CCTA during rest CTP (25 of the 28 volunteers were in the normal group, 3 volunteers and all 4 patients were in the CAD group). All 32 subjects (25 volunteers and 7 patients, 27 men and 5 women, 47.8 ± 9.5 years old) (Fig. 1) underwent both MDCT and ^{15}O-H_2O PET perfusion imaging at rest and with adenosine triphosphate (ATP) stress within a 2-week period.

The normal group was randomized into a pilot group (11 men and 1 woman) to establish the MBF_{CT} calculation method and a validation group (11 men and 2 women) for validation of MBF_{CT} and CFR_{CT} against PET.

Subject Preparation

All subjects refrained from drinking caffeinated beverages for at least 24 hours, eating for more than 6 hours, and smoking for at least 4 hours before MDCT or PET [17].

The blood pressure (BP), heart rate (HR) and electrocardiogram (ECG) were monitored during examinations. The rate-pressure product (RPP) was calculated as systolic BP × HR. The percent change in HR induced by ATP was also calculated.

MDCT Scanning

CTP/CCTA scans were performed using a second-generation 320-row MDCT scanner (Aquilion ONE, ViSION Edition, Toshiba Medical Systems, Otawara, Japan). Preliminary phantom studies were conducted to determine the relationship between the dose of iodinated contrast medium (Iohexol, 350 mgI/ml, Daiichi Sankyo, Tokyo) and CT attenuation.

The MDCT scan protocol is shown in Fig. 2a. Stress dynamic CTP with intravenous ATP infusion (0.16 mg/kg/min) was followed by rest dynamic CTP. For each CTP scan, 50 ml of contrast medium followed by a 30 ml saline chaser was infused at 5 ml/s using a dual-head power injector. A bolus-tracking technique with

real-time image reconstruction was used, with the region of interest (ROI) set in the pulmonary artery trunk and a threshold of 100 HU. After a 5 s delay, dynamic CTP images were acquired for 25 s using the ECG monitoring for prospective triggering with a phase window of only 70-80 % of the R-R interval, not continuous. For dynamic scans, tube voltage = 80 kV, tube current = 120 mA, and gantry rotation time = 275 ms were used. Images were reconstructed at 1 mm intervals using Adaptive Iterative Dose Reduction 3D (AIDR 3D) and beam-hardening correction.

Rest CCTA imaging was performed as a boost scan during rest dynamic CTP, with tube voltage = 80 kV and tube current = 650 mA (for body mass index (BMI) < 22.5) or 800 mA (for BMI ≥ 22.5) at 75 % of the R-R interval with 0.5 mm reconstruction. The boost timing was the peak enhancement time of the left main coronary trunk in stress dynamic CTP.

^{15}O-H_2O PET Scanning

^{15}O-H_2O PET scans were performed as shown in Fig. 2b without ECG gating (ECAT EXACT HR+, Siemens/CTI, Knoxville, TN) [18]. After attenuation correction, rest and stress scans (same ATP dose as for CTP) were performed. For each scan, 1500 MBq of ^{15}O-H_2O was administered intravenously at 2 min at rest, with 20 frames

dynamic PET acquisition initiated over 6 min. ^{15}O-H_2O images were acquired in 2D mode with septa extended.

Quantification of MBF_{PET}

PET images were reconstructed using vendor-supplied filtered back-projection software (ECAT v7.2) with a 10 mm Hann window of the ramp filter. Frames consisted of 63 trans-axial slices (128 × 128 voxels, 3.4 × 3. 4 × 2.4 mm). MBF_{PET} was quantified (mL/min/g) using software developed in-house with left ventricular (LV) chamber and LV myocardium ROIs [18]. MBF_{PET} was quantified as previously described [18-20].

CTP Image Reconstruction and the Formula to Obtain MBF_{CT}

Using multiplanar reformations, rest and stress perfusion images were arranged along the cardiac short axis as 1 mm slices and analyzed quantitatively. Endocardial and epicardial LV ROIs were set manually by a technologist (Y.T.) in three slices (basal, mid, and apical), with those for other slices propagated semiautomatically. Time-attenuation curves (TACs) for the LV chamber and LV myocardium were generated from these ROIs.

The first frame was subtracted from all subsequent frames for each of the stress

and rest TACs. Using the formula derived from the phantom study, the subtracted TAC data was converted to iodine concentrations in the LV myocardium (Ct(t)) and LV chamber (Ca(t)).

Quantitative MBF_{CT} was calculated using a single-tissue compartment model with the Renkin-Crone equation [10,18-20] (See Appendix).

$$dCt(t)/dt = K1 \times Ca(t) - k2 \times Ct(t) \quad \text{Eq.(1)}$$

$$K1 = (1 - \alpha\exp(-\beta/MBF))MBF \quad \text{Eq.(2)}$$

From the measured Ca(t) and Ct(t), $K1_{CT}$ was estimated by curve fitting using the non-linear least squares method. Then, the parameters α and β were estimated by the same method as Eq. (2) using $K1_{CT}$ and $MBF_{PET,}$ assuming that MBF_{CT} equals MBF_{PET} in the same subject.

Parameters α and β were estimated from the data for the pilot group. Then, MBF_{CT} in the validation and CAD groups were calculated using Eq. (2) based on $K1_{CT}$ and estimated α and β.

CFR was also calculated as the ratio of stress MBF to rest MBF [3,21].

$$\text{CFR} = \frac{MBF\_stress}{MBF\_rest} \quad \text{Eq. (3)}$$

CCTA Evaluation

Volume-rendered images, curved multiplanar reformations, maximum-intensity projections, and cross-sectional images were reconstructed from CT angiographic images at a dedicated workstation (Ziostation 2 plus, Ziosoft, Tokyo). All images were visually assessed for stenosis grade in 17 segments [22] and image quality was scored as follows: 4 = excellent (no artifacts), 3 = good (minor artifacts, good diagnostic quality), 2 = adequate (moderate artifacts, acceptable and diagnostic), 1 = poor (severe artifacts impairing accurate evaluation). All assessments were conducted independently by two physicians blinded to all other clinical data, with discrepancies resolved by consensus.

Radiation Dose Calculations

CT radiation doses were estimated using the dose-length product reported by the scanner, with conversion to effective dose by multiplying by a constant (k = 0.014 mSv/mGy/cm) according to the European Guidelines on Quality Criteria for CT [23].

Statistical Analysis

All data are expressed as mean ± SD. The backgrounds of the normal pilot and validation groups were compared using the Student's *t*-test for age and BMI, while

Fisher's exact tests were used for gender and smoking. RPP at rest and % change in HR induced by ATP were compared between CTP and PET using paired *t*-tests.

For comparison of MBF and CFR between CTP and PET, paired *t*-tests, Pearson's correlation coefficients, and linear regression analyses (with Bland-Altman plots) were used. CFRs were compared between the validation and CAD groups using the *t*-test. In addition, receiver operating characteristic (ROC) analysis for detection of CAD was conducted.

Values of $P < 0.05$ were considered statistically significant. JMP® Pro 10 (SAS Institute, Inc., Cary, NC) was used for data analysis.

Results

Subject Characteristics

There were no significant differences in age (46.3 ± 2.5 vs. 44.9 ± 2.4, $P = 0.69$), BMI (22.9 ± 0.7 vs. 22.9 ± 0.6, $P = 0.92$), or smoking history between the pilot and validation groups (Table 1). The CAD group included 5 men and 2 women (56.1 ± 8.7 years) with average BMI 26.8 ± 2.6.

HR increased significantly in stress studies (% change in HR) in both groups for both CTP and PET (for CTP $P = 0.040$, for ^{15}O-H_2O PET $P = 0.021$ in the validation group and $P = 0.009$, $P = 0.002$ in the CAD group respectively) (Table 2). There were no significant differences in baseline RPP or % change in HR between the two modalities in the validation and CAD groups ($P = 0.585$, $P = 0.266$ in the validation group and $P = 0.895$, $P = 0.370$ in the CAD group respectively).

Formula for Computation of MBF_{CT} Using Renkin-Crone Model

The phantom study showed a linear relationship between the contrast medium dose and CT attenuation. The relationship between contrast concentration (x) (mgI/ml) and CT attenuation (HU) (y) was:

$$y = 47.9x + 49.1 \ (r = 1.00) \quad \text{Eq.(4)}$$

Sample TACs from the pilot group after subtraction of the first frame from all subsequent frames (both rest and stress) are shown in Fig. 3. These TACs were converted to contrast concentrations using Eq. (4).

Rest and stress $K1_{CT}$ values in the pilot group were 0.58 ± 0.13 and 1.24 ± 0.17 ml/min/g respectively, and rest and stress MBF_{PET} values were 0.72 ± 0.17 and 3.23 ± 0.73 ml/min/g respectively. From these data, parameters α (0.904) and β (1.203) were estimated using Eq. (2). The Renkin-Crone formula between $K1_{CT}$ and MBF_{CT} was expressed as:

$$K1 = (1 - 0.904\exp(-1.203/MBF_{CT}))MBF_{CT} \quad \text{Eq.(5)}$$

This equation was used to calculate MBF_{CT} in the validation and CAD groups using each subject's $K1_{CT}$.

Validation of MBF_{CT} against ^{15}O-H_2O PET

In the validation group, Pearson's correlation coefficients and linear regression analyses of MBF showed good correlations (r = 0.95, $P < 0.0001$) between CTP and PET (Fig. 4a), but there was a small bias suggesting that MBF_{CT} tended to scatter at high flow seen from the Bland-Altman plot (Fig. 4b). There were no significant differences in rest and stress MBF between CTP and PET in the validation and CAD

groups (for rest $P = 0.831$, for stress $P = 0.757$ in the validation group, and $P = 0.050$, $P = 0.076$ in the CAD group respectively). Stress MBF was significantly higher than rest MBF for CTP and PET (for CTP $P = 0.003$, for PET $P = 0.001$ in the validation group and $P < 0.0001$, $P < 0.0001$ in the CAD group respectively), except for one normal subject in the validation group whose MBF did not increase in the stress study despite refraining from caffeine, smoking, and eating.

Validation and Comparison of CFR between the Validation and the CAD Groups

A moderate correlation was observed in CFR between CTP and PET in the validation group (r = 0.67, $P = 0.0126$) (Fig. 5). CFR_{CT} in the CAD group (2.3 ± 0.8) was significantly lower than in the validation group (5.2 ± 1.8) ($P = 0.0011$) (Fig. 6). CFR_{PET} in the CAD group (2.6 ± 1.1) was also significantly lower than in the validation group (5.0 ± 1.6) ($P = 0.0011$). There were no significant differences between CFR_{CT} and CFR_{PET} in the validation and CAD groups (for validation group $P = 0.81$, for CAD group $P = 0.65$ respectively).

In the ROC analysis of CFR_{CT} for detection of CAD, the area under the curve of the ROC was 0.90 ($P = 0.0043$). The sensitivity was 85.7% and specificity was 92.3%, when a cut-off of 2.97 was used for detection of CAD.

CCTA Image Quality

The average image quality score was 3.8 ± 0.1 for all coronary arteries in all subjects. Only 7 coronary segments (1.6 %) were under score 2 and most coronary segments could be assessed for stenosis (98.4 %). Seventeen coronary segments in 7 patients showed ≥ 50 % stenosis. Five subjects had 1-vessel disease, 1 had 2-vessel disease, and 1 had 3-vessel disease. Curved multiplanar reformation of CCTA and CTP images (stress and rest status) of a CAD patient (BMI 27.7) were shown in Fig. 7. In CCTA image, the image quality of the patient was excellent and the severe stenosis (70-99%) in the proximal of left anterior descending artery (LAD) was well demonstrated. In the left ventricular short axis images of CTP, CT attenuation in the anterior wall (LAD territory) was decreased in the stress CTP.

Radiation Dose

The average total dose for CT studies was 12.8 ± 2.9 mSv for all subjects. That for PET studies was 3.3 mSv according to our past report [24].

Discussion

This study introduced and validated the method for whole MBF and CFR with low dose dynamic 320-row MDCT in comparison with ^{15}O-H_2O PET. Our preliminary results showed that the MBF_{CT} and CFR_{CT} were well correlated with ^{15}O-H_2O PET and lower CFR was well demonstrated in CAD patients compared to normal controls.

It has been hypothesized that combining CCTA and CTP may avoid the limitations of CCTA, allowing the diagnosis of cardiac ischemia with accurate anatomic assessment in one examination. Bettencourt et al. reported that integrating CTP/CCTA improved MDCT performance in detecting clinically significant CAD in intermediate to high pretest probability populations [11]. However, few established protocols have combined stress and rest CTP and CCTA due to the high radiation dose. In addition, incomplete heart coverage as well as motion, beam-hardening, and banding artifacts reduce the accuracy and reproducibility of MBF calculations with 64-row MDCT [16]. Huber et al. reported that the radiation dose in CTP for 25 s with 256-row CT was 9.5 mSv, but only for stress CTP, and they could not calculate CFR [25]. In the present study, for low-dose dynamic CTP in rest and stress status, we scanned at 80 kV instead of 120 kV (as used in a previous study with 320-row MDCT [26]). The average total radiation dose was therefore 12.8 mSv, about half the previous value of 25.5 mSv [26].

At 80 kV, there was no beam-hardening or banding artifact with our protocol, both dynamic LV blood and myocardial TACs were successfully obtained, as well as rest CCTA data. The images of rest CCTA during CTP (HR = 61 ± 8 bpm) were quite good, sufficient for evaluation (average score = 3.8, 98.4 % of segments assessable) [21].

We led the formula and calculated the MBF_{CT} and CFR_{CT} from low dose dynamic CTP, which showed good correlation with ^{15}O-H_2O PET. ^{15}O-H_2O PET has been known as a gold standard for a quantitative assessment of the MBF, because ^{15}O-H_2O PET is the only one that a freely diffusible tracer with 100% extraction fraction even at increased blood flows [10]. The extraction fraction in other tracers are lower than that of ^{15}O-H_2O PET [10]. This study was the first article where MBF and CFR calculated from CTP were validated by ^{15}O-H_2O PET.

CFR has been used as a sensitive marker of high-risk anatomic coronary artery disease in a PET study [27], but PET cannot provide coronary morphological information with MBF and CFR simultaneously. Our 320-row MDCT comprehensive protocol provides quantitative MBF and CFR together with morphological information. Clinically, CFR_{CT} may help in evaluating the functional severity of CAD, especially with severe calcification, which interferes with CCTA evaluation [1]. CFR_{CT} in CAD patients were significantly lower than normal controls in this study. In addition, the

sensitivity was 85.7% and specificity was 92.3% at a cut-off value of 2.97 for detection of CAD. CFR cut-off values have generally been 2.0 or 2.5, scores found useful for predicting outcome or microcirculatory dysfunction [5-9].

Our method employing both K1 and k2 is more complicated than the Patlak plot and upslope methods, which do not consider k2 (the outflow rate from LV myocardium into the LV chamber) and do not require the entire TAC [28,29]. MBF values are systematically underestimated, especially at high flow with the Patlak plot and upslope methods [28,29]. Therefore, our method with K1 and k2 is more physiologic for calculating MBF.

In this study, there was a small bias suggesting that MBF_{CT} tended to scatter at high flow during stress as compared to PET. This may have been due to different reactions to pharmacological stress in individual subjects. However, the correlations of MBF and CFR between the two modalities were quite high, indicating MBF_{CT} and CFR_{CT} are reliable indicators.

This study has several limitations. First, the order of rest and stress scans differed between the two modalities. Stress CTP was performed before rest CTP/CCTA because rest CTP/CCTA requires the pre-scan administration of nitrates and/or beta-blockers, which might mask myocardial ischemia in subsequent stress CTP. In addition, the

optimal boost timing for rest CCTA was determined using stress CTP data. Therefore, the timing of boosted CCTA during rest CTP was good and resulted in good image quality. On the other hand, PET scans were performed in the opposite order to save time. We think this did not significantly affect the results, because the RPPs were not significantly different between the two modalities and a previous study reported no effects on MBF_{PET} with different scan orders [30]. In addition, we subtracted the first frame from all subsequent frames in both stress and rest CTP so the residual contrast from the stress scan would not affect the subsequent rest scan.

Second, only the whole MBF, not regional MBF, was calculated. In general, whole MBF and CFR are of utility in relatively limited populations. In addition, it would be possible to match the culprit site of CCTA with the ischemic lesion of CTP by calculating the regional MBF. However, this is a preliminary study and the study showed the potential for detecting myocardial ischemia using only MDCT. In this study, regional MBF cannot be obtained due to unstable curve fitting for estimating K1 and higher noise in low-dose CTP. More effective noise reduction using iterative image reconstruction or other techniques may allow assessment of regional MBF.

Finally, over-weight or female subjects were not included in this study, which may have resulted in an under- or overestimation of the radiation dose that would normally be seen in a typical patient population including female or overweight to obese subjects.

In conclusion, we have established a method for calculating whole MBF and CFR using low-dose dynamic CTP scanning with 320-row MDCT with validation against ^{15}O-H_2O PET. This method may provide comprehensive clinical information regarding quantitative MBF, CFR, and coronary artery stenosis with low-dose MDCT.

Appendix

For quantitative analysis, we used the single-tissue compartment model and differential equations from the whole TACs of the LV blood and myocardium for calculation of K1 and k2.

The following equation was used for robust estimation of inflow rate (K1) of contrast media into Ct(t),

$$dCt(t)/dt = K1 \times Ca(t) - k2 \times Ct(t) \quad (1)$$

where k2 is the outflow rate from LV myocardium into the LV blood cavity. The relationship of MBF and K1 of iodine contrast media of MDCT is given by the Renkin-Crone model as,

$$K1 = MBF \times E \quad (2)$$

where E is an extraction fraction specific a certain tracer or contrast media. This E has nonlinear relationship with MBF and the effective capillary permeability × surface-area product (PS, mL/min/g).

$$E = 1 - e^{-PS/MBF} \quad (3)$$

This model is consistent with the observation that tracer or contrast media extraction typically decreases with flow, despite the PS product increasing due to capillary recruitment. The PS function is typically presented as,

$$PS = A \times MBF + \beta \quad (4)$$

using (2), (3), and (4), the Renkin Crone model was expressed as ;

$$K1 = (1 - \alpha\exp(-\beta/MBF))MBF \quad (5)$$

where “α” is exp (-A).

References

1 Miller JM, Rochitte CE, Dewey M, et al. (2008) Diagnostic performance of coronary angiography by 64-row CT. The New England journal of medicine, 359(22):2324-2336

2 Uren NG, Melin JA, De Bruyne B, Wijns W, Baudhuin T, Camici PG (1994) Relation between myocardial blood flow and the severity of coronary-artery stenosis. The New England journal of medicine, 330(25):1782-1788

3 Camici PG, Crea F (2007) Coronary microvascular dysfunction. The New England journal of medicine, 356(8):830-840

4 Naya M, Murthy VL, Blankstein R, et al. (2011) Quantitative relationship between the extent and morphology of coronary atherosclerotic plaque and downstream myocardial perfusion. Journal of the American College of Cardiology, 58(17):1807-1816

5 Daimon M, Watanabe H, Yamagishi H, et al. (2001) Physiologic assessment of coronary artery stenosis by coronary flow reserve measurements with transthoracic Doppler echocardiography: comparison with exercise thallium-201 single piston emission computed tomography. Journal of the American College of Cardiology, 37(5):1310-1315

6 Miller DD, Donohue TJ, Younis LT, et al. (1994) Correlation of pharmacological 99mTc-sestamibi myocardial perfusion imaging with poststenotic coronary flow reserve in patients with angiographically intermediate coronary artery stenoses. Circulation, 89(5):2150-2160

7 Tron C, Donohue TJ, Bach RG, et al. (1995) Comparison of pressure-derived fractional flow reserve with poststenotic coronary flow velocity reserve for prediction of stress myocardial perfusion imaging results. American heart journal, 130(4):723-733

8 Matsumura Y, Hozumi T, Watanabe H, et al. (2003) Cut-off value of coronary flow velocity reserve by transthoracic Doppler echocardiography for diagnosis of significant left anterior descending artery stenosis in patients with coronary risk factors. The American journal of cardiology, 92(12):1389-1393

9 Kawata T, Daimon M, Hasegawa R, et al. (2013) Prognostic value of coronary flow reserve assessed by transthoracic Doppler echocardiography on long-term outcome in asymptomatic patients with type 2 diabetes without overt coronary artery disease. Cardiovascular diabetology, 12(1):121

10 Klein R, Beanlands RS, deKemp RA (2010) Quantification of myocardial blood flow

and flow reserve: Technical aspects. Journal of nuclear cardiology : official publication of the American Society of Nuclear Cardiology, 17(4):555-570

11 Bettencourt N, Chiribiri A, Schuster A, et al. (2013) Direct comparison of cardiac magnetic resonance and multidetector computed tomography stress-rest perfusion imaging for detection of coronary artery disease. Journal of the American College of Cardiology, 61(10):1099-1107

12 Vavere AL, Simon GG, George RT, et al. (2011) Diagnostic performance of combined noninvasive coronary angiography and myocardial perfusion imaging using 320 row detector computed tomography: design and implementation of the CORE320 multicenter, multinational diagnostic study. Journal of cardiovascular computed tomography, 5(6):370-381

13 George RT, Arbab-Zadeh A, Miller JM, et al. (2012) Computed tomography myocardial perfusion imaging with 320-row detector computed tomography accurately detects myocardial ischemia in patients with obstructive coronary artery disease. Circulation. Cardiovascular imaging, 5(3):333-340

14 Roger VL, Go AS, Lloyd-Jones DM, et al. (2012) Heart disease and stroke statistics--2012 update: a report from the American Heart Association. Circulation, 125(1):e2-e220

15 So A, Wisenberg G, Islam A, et al. (2012) Non-invasive assessment of functionally relevant coronary artery stenoses with quantitative CT perfusion: preliminary clinical experiences. European radiology, 22(1):39-50

16 Kitagawa K, George RT, Arbab-Zadeh A, Lima JA, Lardo AC (2010) Characterization and correction of beam-hardening artifacts during dynamic volume CT assessment of myocardial perfusion. Radiology, 256(1):111-118

17 Morita K, Tsukamoto T, Naya M, et al. (2006) Smoking cessation normalizes coronary endothelial vasomotor response assessed with 15O-water and PET in healthy young smokers. Journal of nuclear medicine : official publication, Society of Nuclear Medicine, 47(12):1914-1920

18 Katoh C, Morita K, Shiga T, Kubo N, Nakada K, Tamaki N (2004) Improvement of algorithm for quantification of regional myocardial blood flow using 15O-water with PET. Journal of nuclear medicine : official publication, Society of Nuclear Medicine, 45(11):1908-1916

19 Herrero P, Markham J, Shelton ME, Bergmann SR (1992) Implementation and evaluation of a two-compartment model for quantification of myocardial perfusion with rubidium-82 and positron emission tomography. Circulation research, 70(3):496-507

20 Katoh C, Yoshinaga K, Klein R, et al. (2012) Quantification of regional myocardial blood flow estimation with three-dimensional dynamic rubidium-82 PET and modified spillover correction model. Journal of nuclear cardiology : official publication of the American Society of Nuclear Cardiology, 19(4):763-774

21 Yoshinaga K, Chow BJ, dekemp RA, et al. (2005) Application of cardiac molecular imaging using positron emission tomography in evaluation of drug and therapeutics for cardiovascular disorders. Current pharmaceutical design, 11(7):903-932

22 Raff GL, Abidov A, Achenbach S, et al. (2009) SCCT guidelines for the interpretation and reporting of coronary computed tomographic angiography. Journal of cardiovascular computed tomography, 3(2):122-136

23 Cousins C, Miller DL, Bernardi G, et al. (2013) ICRP PUBLICATION 120: Radiological protection in cardiology. Annals of the ICRP, 42(1):1-125

24 deKemp RA, Yoshinaga K, Beanlands RS (2007) Will 3-dimensional PET-CT enable the routine quantification of myocardial blood flow? Journal of nuclear cardiology : official publication of the American Society of Nuclear Cardiology, 14(3):380-397

25 Huber AM, Leber V, Gramer BM, et al. (2013) Myocardium: Dynamic versus Single-Shot CT Perfusion Imaging. Radiology

26 George RT, Arbab-Zadeh A, Cerci RJ, et al. (2011) Diagnostic performance of combined noninvasive coronary angiography and myocardial perfusion imaging using 320-MDCT: the CT angiography and perfusion methods of the CORE320 multicenter multinational diagnostic study. AJR. American journal of roentgenology, 197(4):829-837

27 Crone C (1963) The Permeability of Capillaries in Various Organs as Determined by Use of the 'Indicator Diffusion' Method. Acta physiologica Scandinavica, 58:292-305

28 George RT, Jerosch-Herold M, Silva C, et al. (2007) Quantification of myocardial perfusion using dynamic 64-detector computed tomography. Investigative radiology, 42(12):815-822

29 Ichihara T GR, Lima JAC (2010) Evaluation of Equivalence of Upslope Method-Derived Myocardial Perfusion Index and Transfer Constant Based on Two-Compartment Tracer Kinetic Model for CT Quantitative Myocardial Perfusion(ed)^(eds) Nuclear Science Symposium Conference Record, pp 2330-2333

30 Furuyama H, Odagawa Y, Katoh C, et al. (2003) Altered myocardial flow reserve and endothelial function late after Kawasaki disease. The Journal of pediatrics, 142(2):149-154

Figure Legends

Figure 1.

Enrollment of Subjects

Two volunteers out of 34 subjects were excluded because MDCT protocol was not fully completed. Therefore, total 32 subjects were enrolled and divided into 3 groups; normal pilot (n = 12), normal validation (n = 13), and coronary artery disease (CAD) (n = 7) groups.

Figure 2.

Flowchart of Image Acquisition Methods

a. MDCT scan protocol

First, the stress dynamic computed tomography perfusion (CTP) imaging was performed during the intravenous infusion of adenosine triphosphate (ATP) (0.16 mg/kg/min) under the continuous ECG monitoring. Three minutes after starting the ATP infusion, 50 ml of iodine contrast media was infused at a flow rate of 5 ml/s using a dual-head power injector, followed by 30 ml saline chaser at the same rate. ATP infusion had been continued until the stress dynamic CTP scan was finished. Second, the rest dynamic CTP/cardiac computed tomography angiography (CCTA) imaging was

performed at least 15 min after the stress dynamic CTP. We used an intravenous propranolol (up to 10 mg) if the HR for rest CCTA was greater than 65 beats per minutes (bpm).

b. ^{15}O-H_2O PET scan protocol

We undergo ^{15}O-H_2O PET scans at rest and stress status without ECG gating. Pharmacological stress is induced using the same dose of ATP as CTP. For each scan, 1500 MBq of ^{15}O-H_2O was administered intravenously at 2 min at rest.

Figure 3.

Time Attenuation Curves (TACs) of CT Perfusion at Rest and Stress Status

The subtracted TACs, at rest (a) and at stress (b), which are subtracted the first frame from all frames are shown. The dotted lines show TACs of the left ventricular (LV) blood cavities and the continuous lines show TACs of the LV myocardium.

Figure 4.

The Relationship between MBF_{CT} and MBF_{PET} in the Validation Group

Black circle is at rest and white triangle is at stress status.

a. Correlation and Linear Regression Analysis between MBF_{CT} and MBF_{PET}

Pearson's correlation coefficients and linear regression analyses of MBF show good and significant correlation (r = 0.95, $P < 0.0001$) between CT perfusion and ^{15}O-H_2O PET.

b. Bland Altman Plot between MBF_{CT} and MBF_{PET}

There is a small bias (mean 0.08) suggesting MBF_{CT} tended to scatter at high flow in the variation group. However, it is within ± 1.96 SD limits of agreement between two modalities.

Figure 5.

The Relationship between CFR_{CT} and CFR_{PET}

The linear regression analysis of CFR between CT perfusion and ^{15}O-H_2O PET in the validation group show moderate and significant correlation (r = 0.67, $P = 0.0126$).

Figure 6.

Comparison between The Validation Group with No Coronary Artery Stenosis and The Coronary Artery Disease Group with Coronary Artery Stenosis for Each CFR_{CT} and CFR_{PET}

The black circle is CFR_{PET} and black triangle is CFR_{CT}. There are no significant differences between CFR_{CT} and CFR_{PET} in each validation and coronary artery disease (CAD) group. Both CFR_{CT} (2.3 ± 0.8) and CFR_{PET} (2.6 ± 1.1) in the CAD group are

significantly lower than those (5.2 ± 1.8, 5.0 ± 1.6 respectively) in the validation group (P = 0.0011 and P = 0.0011 respectively).

Figure 7.

Example of cardiac computed tomography angiography (CCTA) image taken during rest CT perfusion (CTP) image

The patient was 43 y.o. man and his BMI was 27.7. Curved planar reconstruction of (a) the left anterior descending artery (LAD) was shown. The image quality of CCTA was excellent and the severe stenosis (70-99%) of the proximal of the LAD is clearly demonstrated (arrow head). In the stress CTP status, CT attenuation in the anterior wall (LAD territory) was decreased (b). On the other hand, the CT attenuation in the same area was normal in the rest CTP (c). Note that there was no beam-hardening or banding artifact of the CTP.

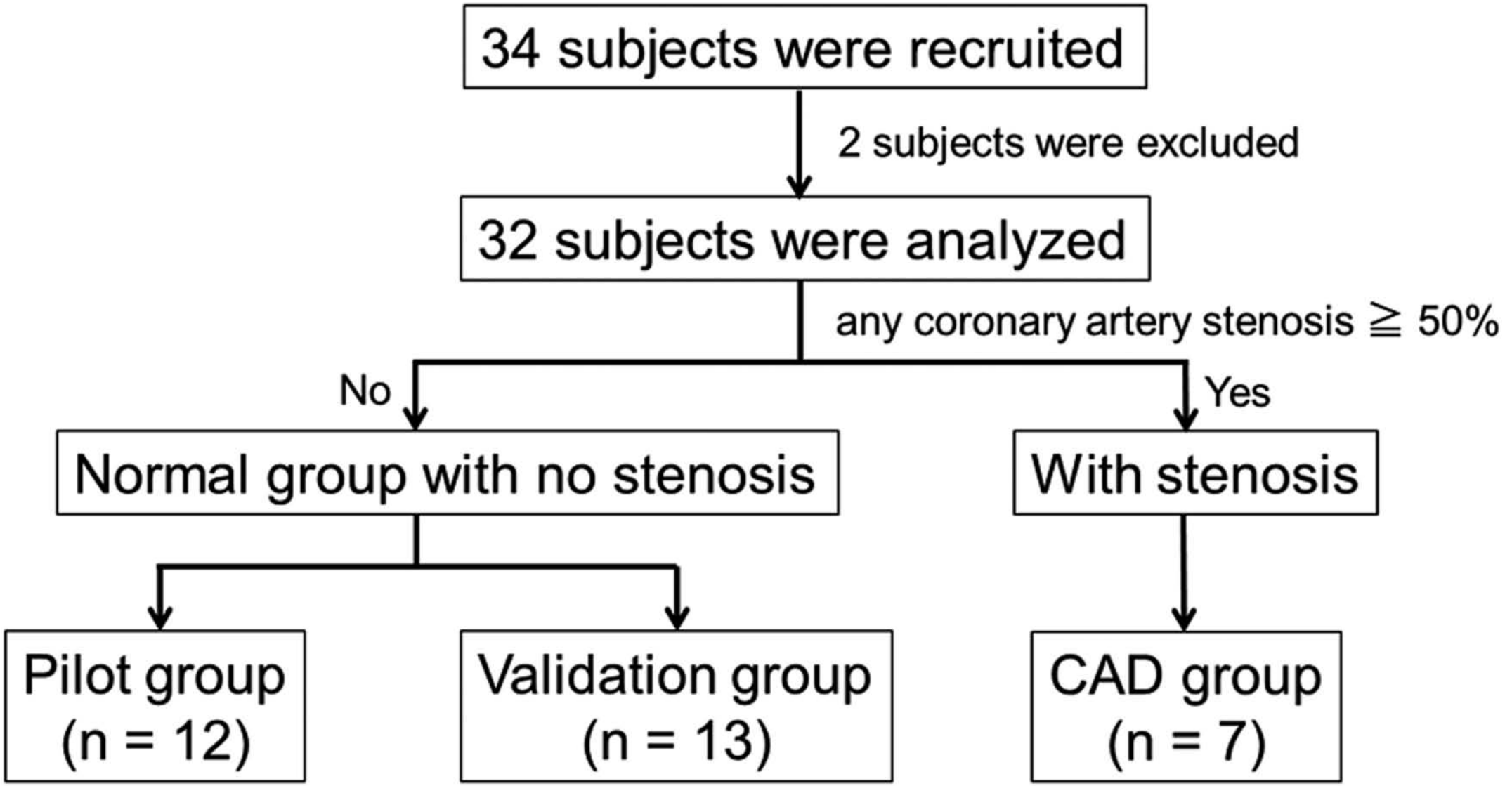
34 subjects were recruited
2 subjects were excluded
32 subjects were analyzed
any coronary artery stenosis ≧ 50%
No
Yes
Normal group with no stenosis
With stenosis
Pilot group
(n = 12)
Validation group
(n = 13)
CAD group
(n = 7)

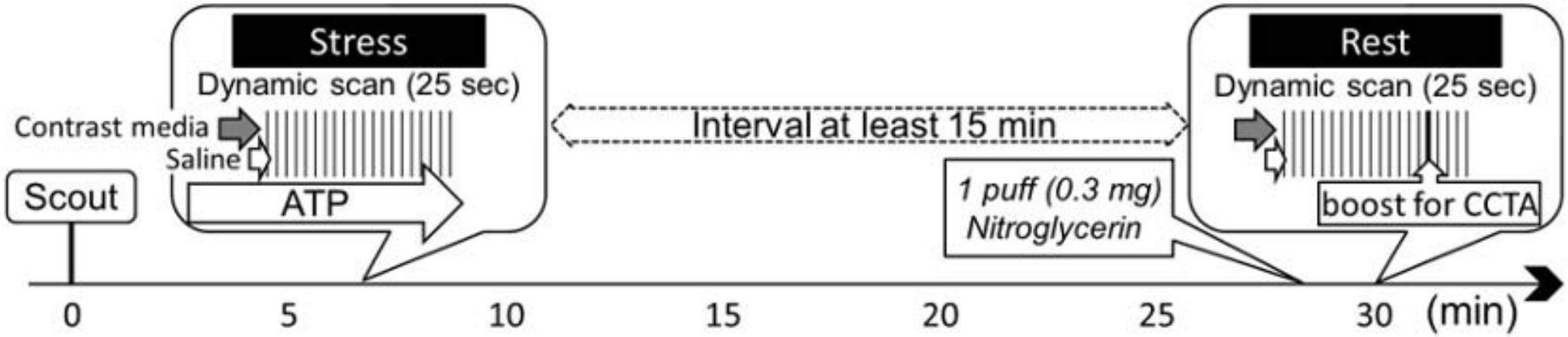
Stress
Dynamic scan (25 sec)
Contrast media
Saline
ATP
Scout
Interval at least 15 min
1 puff (0.3 mg)
Nitroglycerin
Rest
Dynamic scan (25 sec)
boost for CCTA
0
5
10
15
20
25
30
(min)

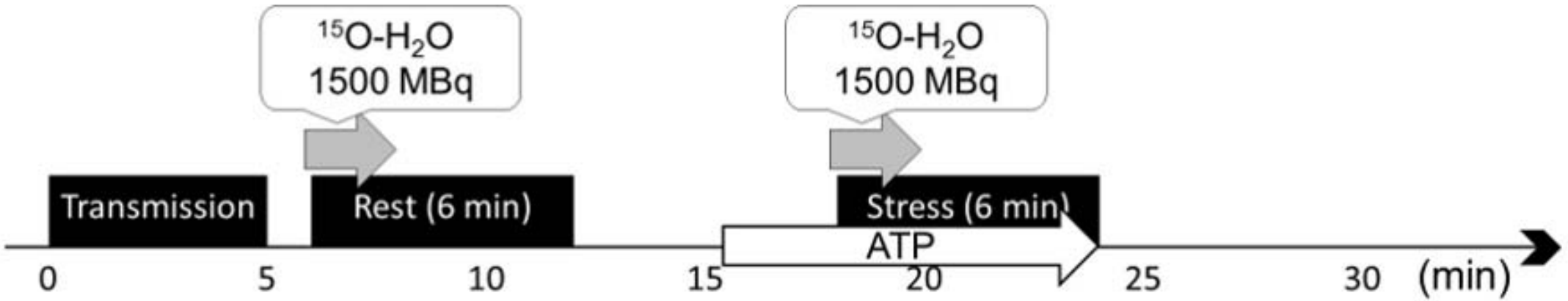
^{15}O-H_2O
1500 MBq
^{15}O-H_2O
1500 MBq
Transmission
Rest (6 min)
Stress (6 min)
ATP
0
5
10
15
20
25
30
(min)

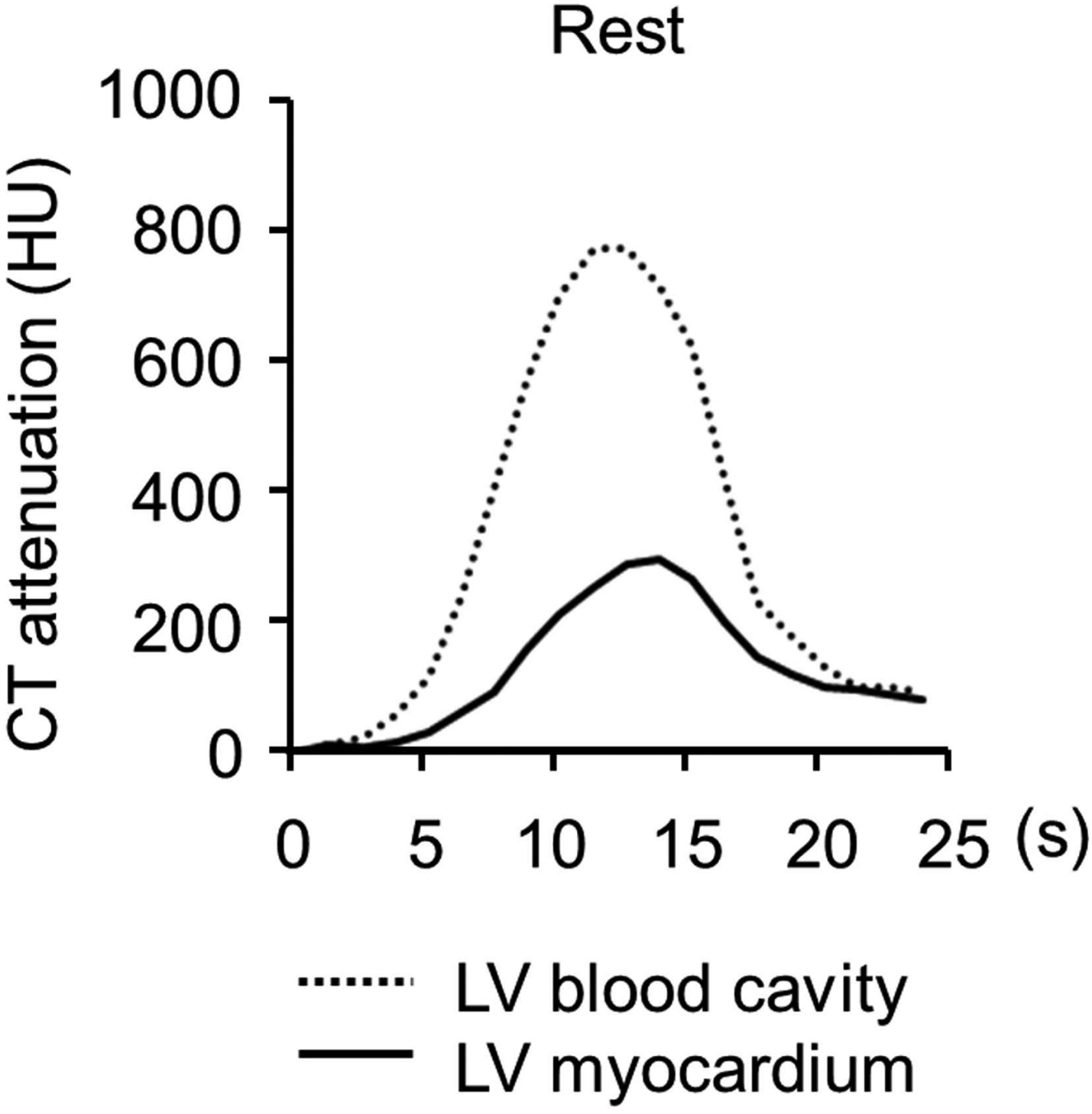
Rest
1000
800
600
400
200
0
CT attenuation (HU)
0
5
10
15
20
25
(s)
LV blood cavity
LV myocardium

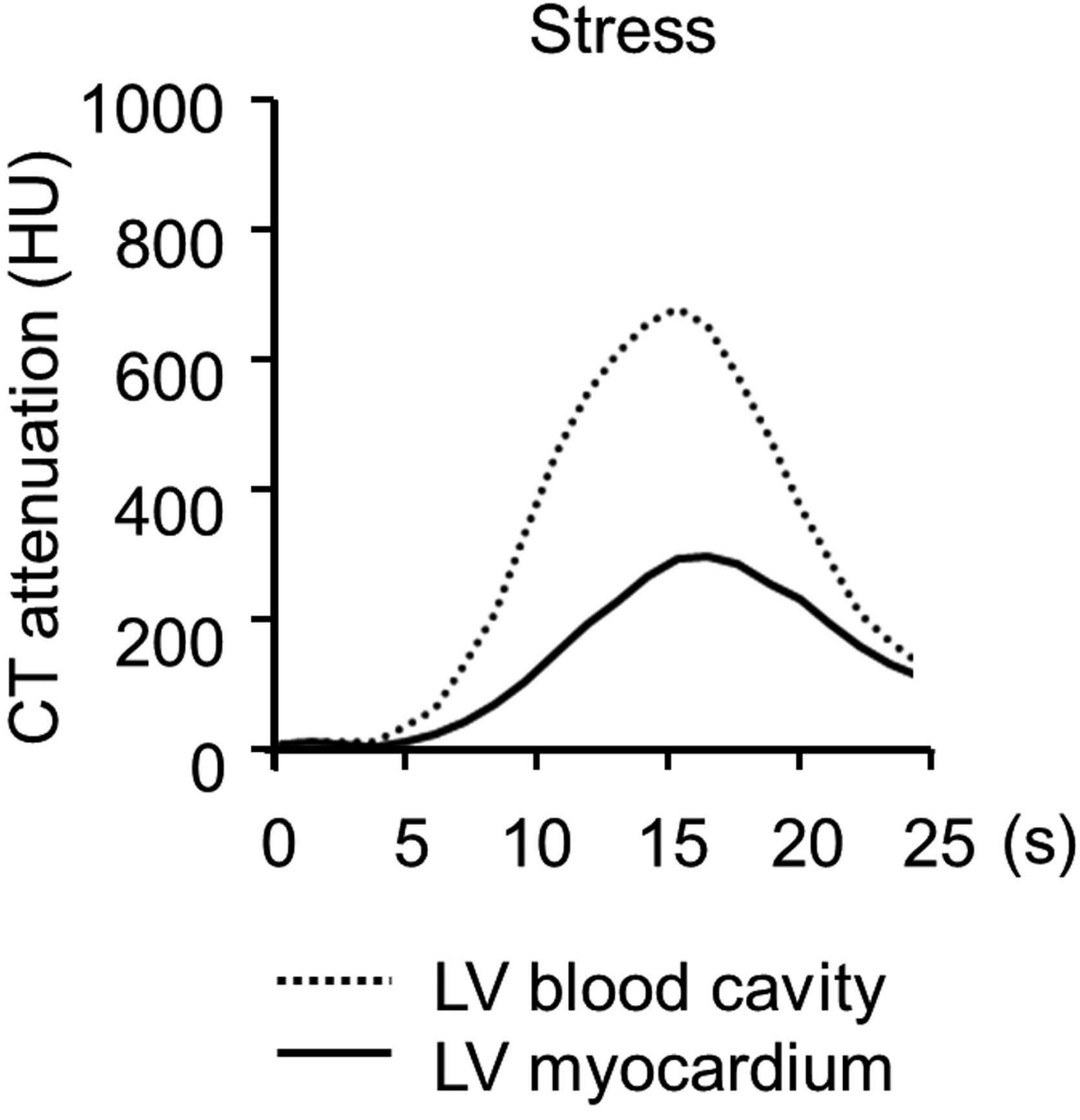
Stress
CT attenuation (HU)
1000
800
600
400
200
0
0
5
10
15
20
25 (s)
LV blood cavity
LV myocardium

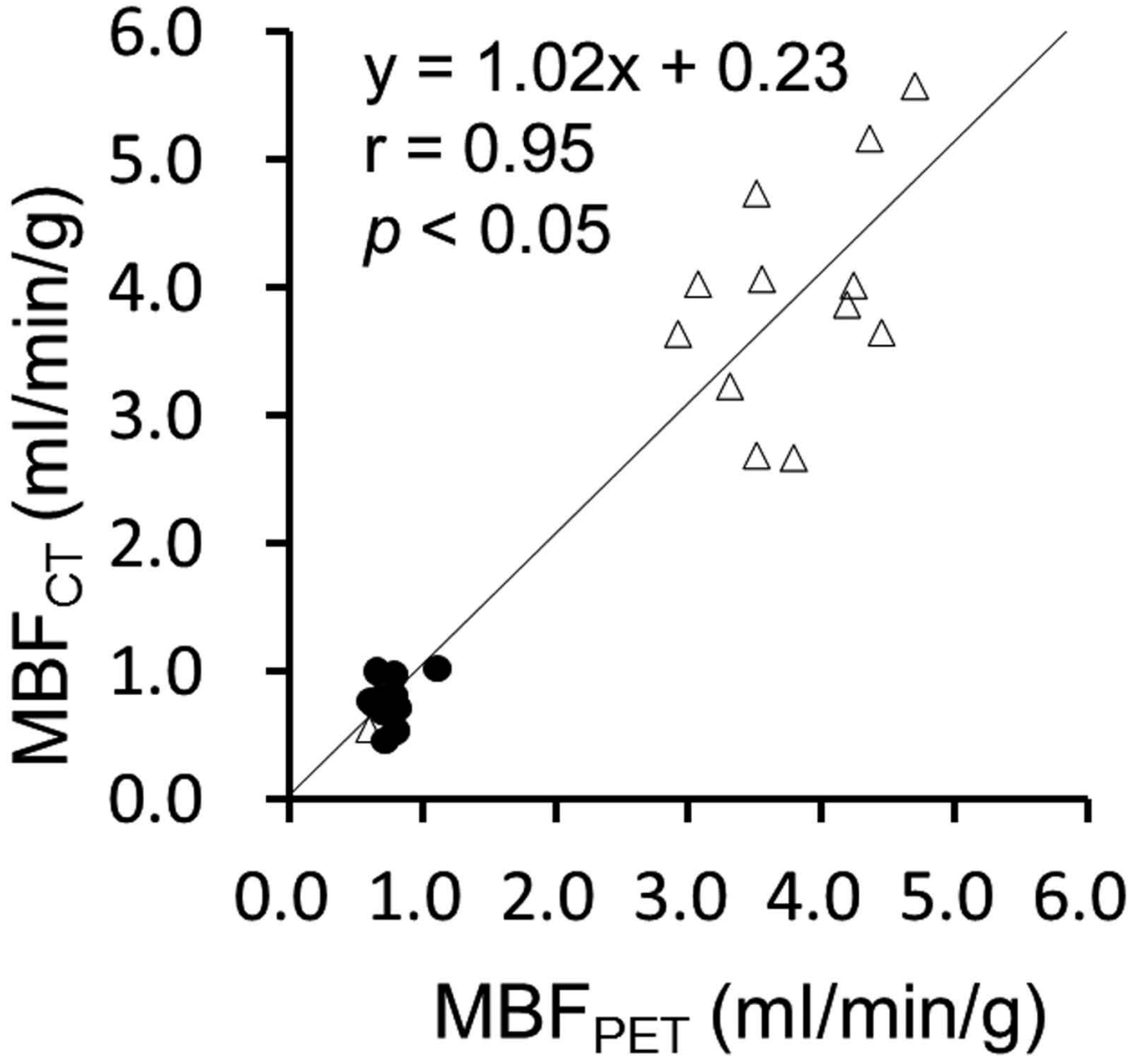
y = 1.02x + 0.23
r = 0.95
p < 0.05
MBF_CT (ml/min/g)
MBF_PET (ml/min/g)
0.0
1.0
2.0
3.0
4.0
5.0
6.0
●: at rest status
△: at stress status

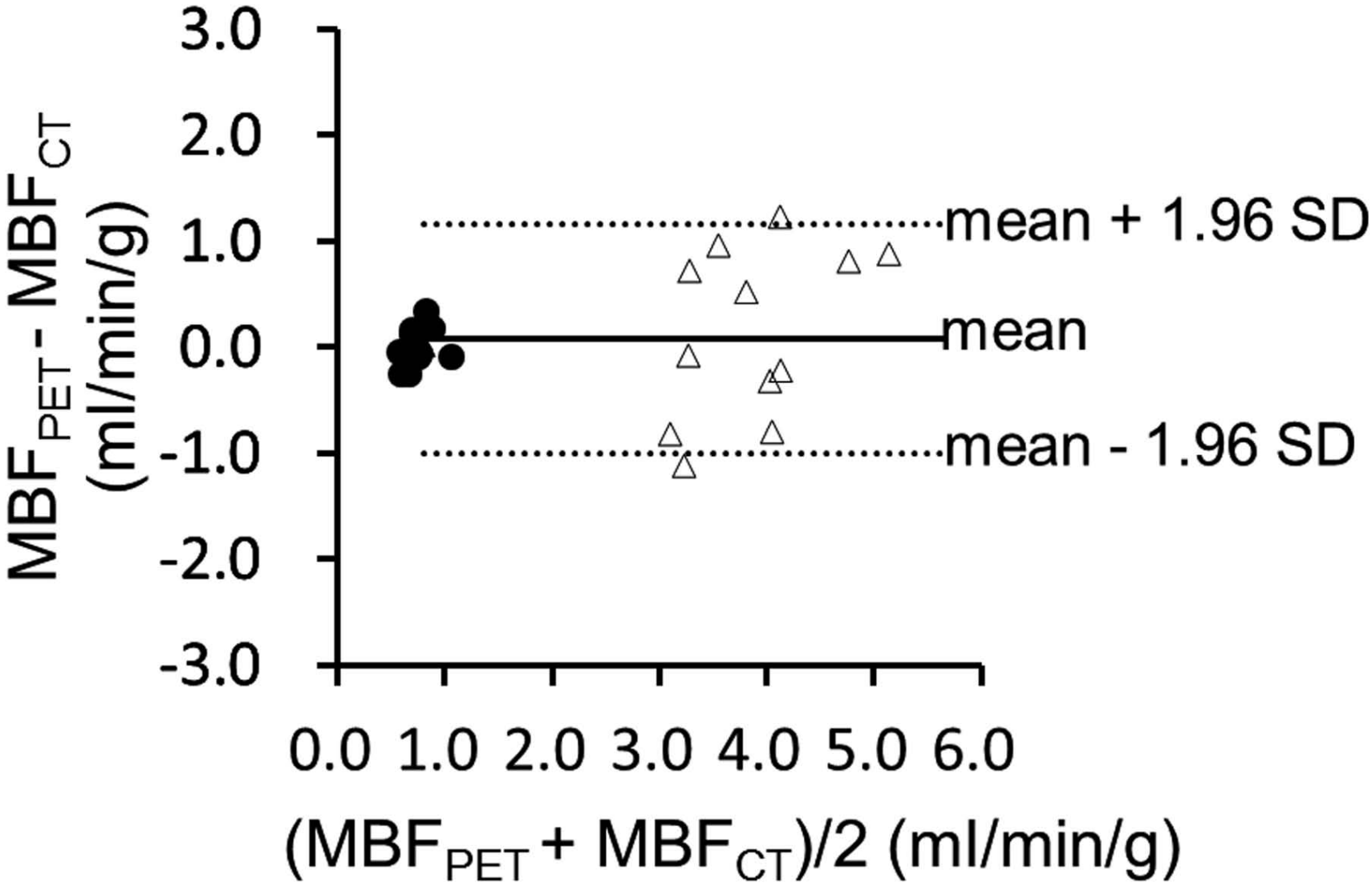

●: at rest status

△: at stress status

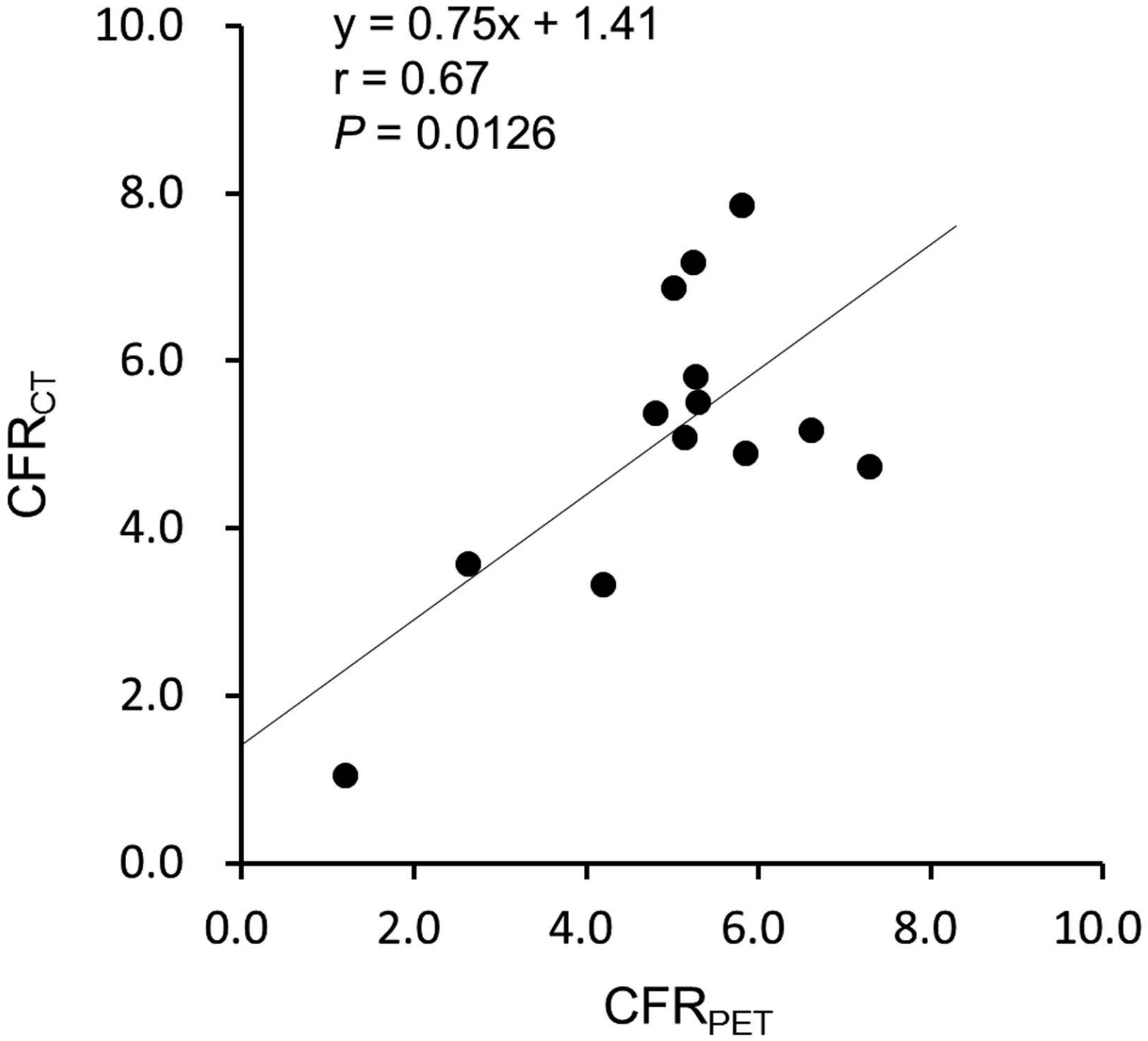
y = 0.75x + 1.41
r = 0.67
P = 0.0126
10.0
8.0
6.0
4.0
2.0
0.0
CFR_CT
0.0
2.0
4.0
6.0
8.0
10.0
CFR_PET

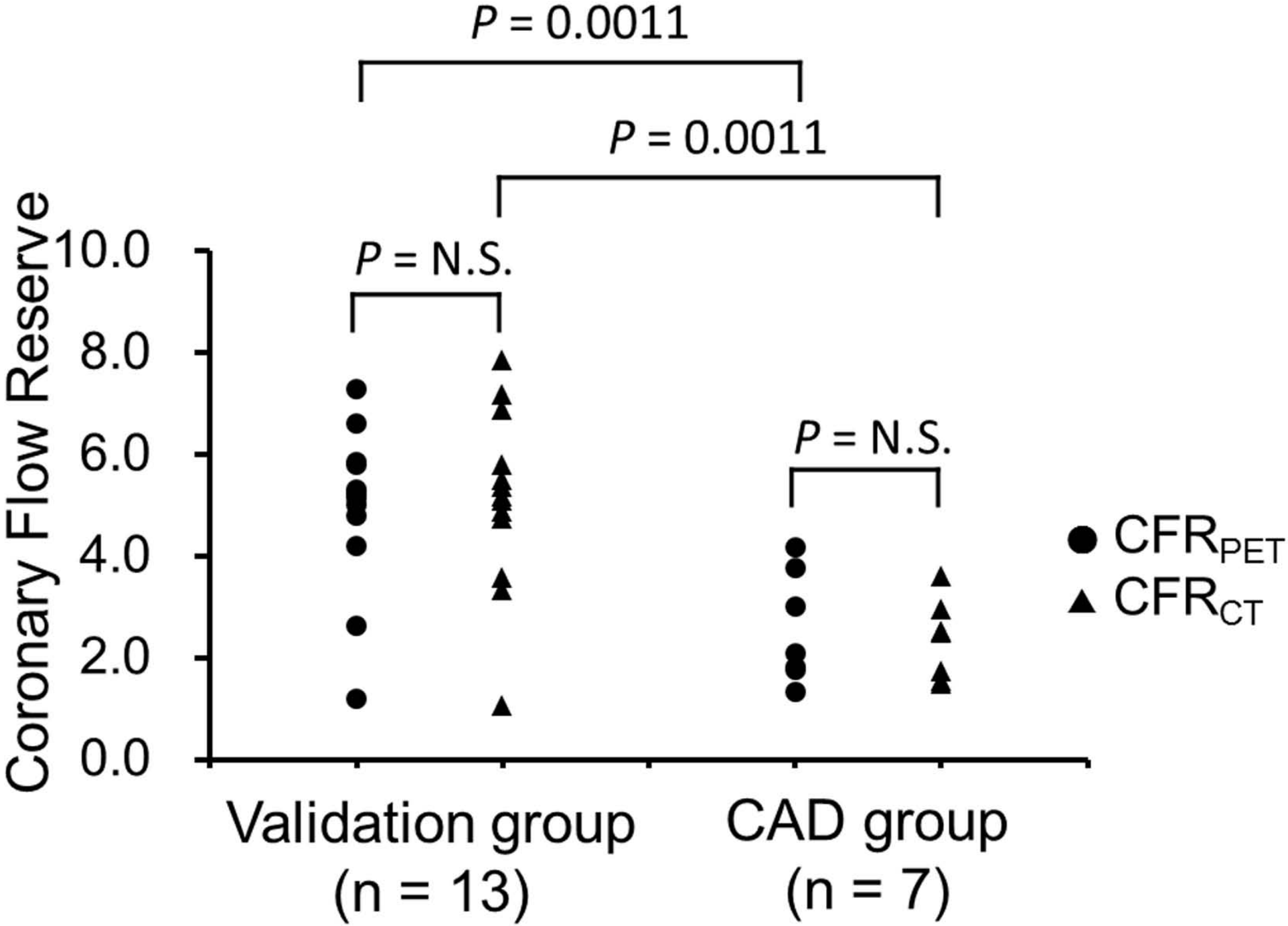
P = 0.0011
P = 0.0011
P = N.S.
P = N.S.
Coronary Flow Reserve
10.0
8.0
6.0
4.0
2.0
0.0
CFR_PET
CFR_CT
Validation group
(n = 13)
CAD group
(n = 7)


Stress

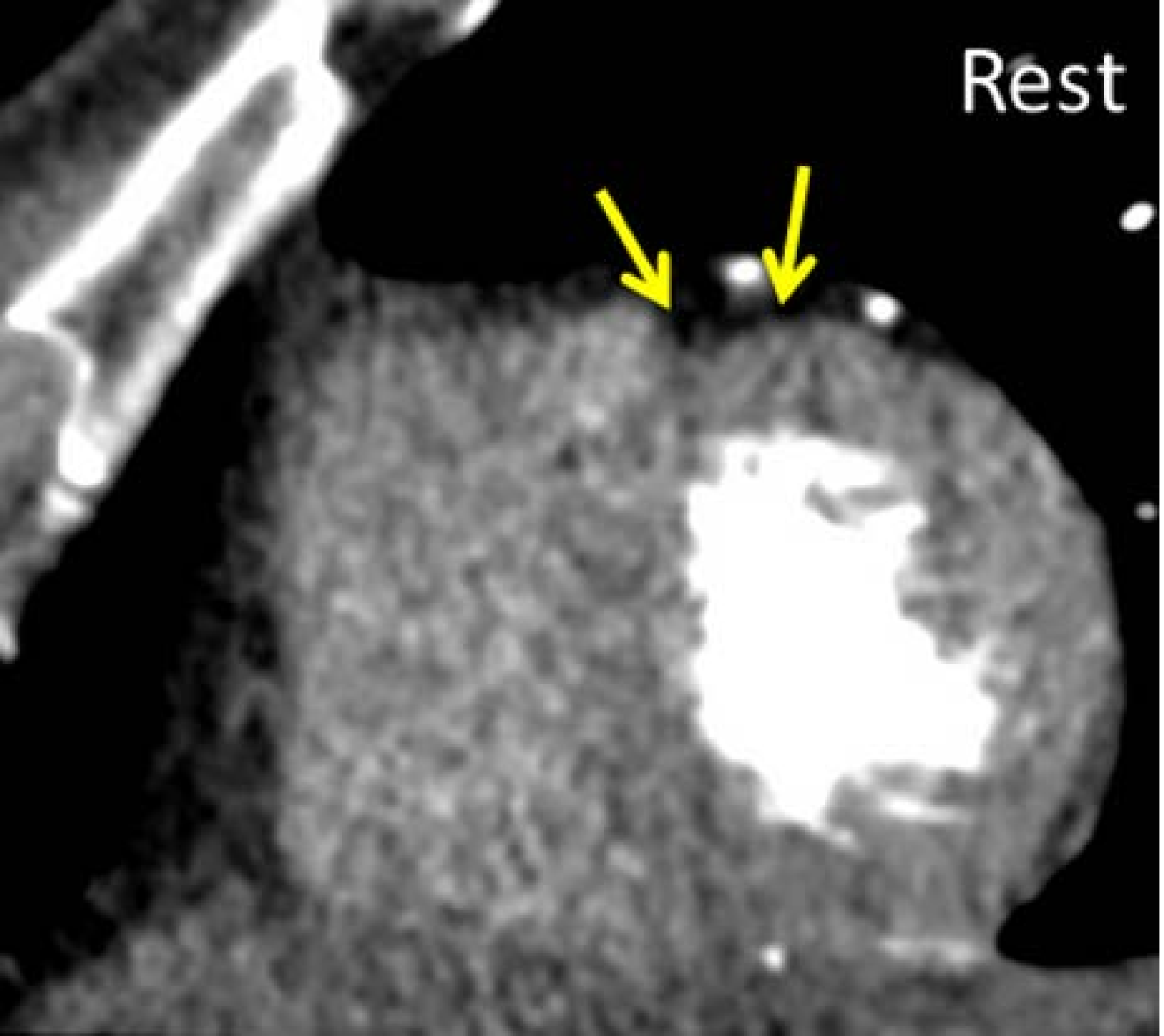
Rest

Table 1. Baseline Characteristics

	Pilot group (n = 12)	Validation group (n = 13)	CAD group (n = 7)
Age(years)	46.3 ± 8.7	44.8 ± 8.5	56.1 ± 8.7
Gender(Man/Woman)	11/1	11/2	5/2
BMI	22.9 ± 2.1	22.8 ± 2.4	26.8 ± 2.6
Smoking	3	3	4
Vessel disease (VD) in CTA			
0-VD	12	13	
1-VD			5
2-VD			1
3-VD			1

Data expressed as mean ± SD; CAD: coronary artery disease; BMI: body mass index; VD: vessel disease; CTA: computed tomography angiography. There were no significant differences in all markers between the pilot and validation groups.

Table 2. Hemodynamics

	Pilot Group (n = 12)		Validation Group (n = 13)		CAD Group (n = 7)	
	CTP	^{15}O-H_2O PET	CTP	^{15}O-H_2O PET	CTP	^{15}O-H_2O PET
Rest status						
sBP (mmHg)	104 ± 11	102 ± 10	105 ± 15	105 ± 12	124 ± 9	129 ± 18
HR (/min)	60 ± 7	58 ± 8	59 ± 8	61 ± 13	68 ± 7	65 ± 9
RPP (mmHg/min)	6259 ± 889	5994 ± 1175	6141 ± 1210	6439 ± 1518	8484 ± 1247	8366 ± 1962
Stress status						
sBP (mmHg)	105 ± 12	96 ± 13	105 ± 16	101 ± 13	124 ± 12	116 ± 11
HR (/min)	78 ± 13	71 ± 11	76 ± 13	73 ± 12	84 ± 9	83 ± 8
% change	18 ± 9	17 ± 7	16 ± 10	21 ± 12	22 ± 9	30 ± 19

CAD: coronary artery disease; CTP: computed tomography perfusion; sBP: systolic blood pressure; HR: heart rate; min: minute; RPP: rate pressure product; % changes: per cent changes in HR before and after adenosine triphosphate infusion.